Mathematical Modelling and Analysis
Volume 29, Issue 3, 560–574, 2024
https://doi.org/10.3846/mma.2024.20905

Stability of the Higher-Order Splitting Methods for the Nonlinear Schrödinger Equation with an Arbitrary Dispersion Operator

Shalva Amiranashvili[a] **and Raimondas Čiegis**[b]

[a] *Weierstrass Institute*
Mohrenstrasse 39, 10117 Berlin, Germany
[b] *Vilnius Gediminas Technical University*
Sauletekio al. 11, 10223 Vilnius, Lithuania
E-mail(*corresp.*): shalva.amiranashvili@wias-berlin.de
E-mail: raimondas.ciegis@vilniustech.lt

Received January 30, 2024; accepted May 16, 2024

Abstract. The numerical solution of the generalized nonlinear Schrödinger equation by simple splitting methods can be disturbed by so-called *spurious instabilities*. We analyze these numerical instabilities for an arbitrary splitting method and apply our results to several well-known higher-order splittings. We find that the spurious instabilities can be suppressed to a large extent. However, they never disappear completely if one keeps the integration step above a certain limit and applies what is considered to be a more accurate higher-order method. The latter can be used to make calculations more accurate with the same numerically stable step, but not to make calculations faster with a much larger step.

Keywords: nonlinear optics, nonlinear fibers, nonlinear Schrödinger equation, generalized nonlinear Schrödinger equation (GNLSE), modulation instability (MI), four-wave mixing, spurious instabilities, splitting methods.

AMS Subject Classification: 78A40; 78A60; 91G60.

1 Introduction

The dynamics of many natural systems can be viewed as the evolution of a modulated weakly nonlinear carrier wave, where the modulation evolves on a much larger time scale than the carrier wave itself [12, 26]. A typical example is a wave packet that contains many field oscillations and whose envelope slowly

evolves in a frame propagating at the carrier group velocity $v_{\rm gr}$. Slow means slow compared to $2\pi/\omega_0$ for the carrier wave at circular frequency $\omega = \omega_0$. Taking advantage of scale separation, one derives a simplified propagation equation for the complex wave amplitude ψ, see [20, 27]. For example, in the context of nonlinear optical fibers the envelope $\psi = \psi(z, \tau)$ depends on the spatial coordinate z along the fiber and the retarded time $\tau = t - z/v_{\rm gr}$. The resulting generalized nonlinear Schrödinger equation (GNLSE) refers to the co-moving frame and reads [1, 8]

$$i\partial_z\psi + \mathfrak{D}(\psi) + \gamma|\psi|^2\psi = 0, \qquad \mathfrak{D}(e^{-i\mathcal{W}\tau}) = D(\mathcal{W})e^{-i\mathcal{W}\tau}. \tag{1.1}$$

Here $\mathfrak{D}$ is the so-called *dispersion operator* with the characteristic function $D(\mathcal{W})$ and γ is a material constant that quantifies the presupposed Kerr nonlinearity. For certainty we will consider γ to be positive, as it is in most cases [4].

The frequency parameter $\mathcal{W}$ is associated with the retarded time τ. If the latter is discretized with the step $\Delta\tau$, one is dealing with the finite bandwidth, approximate solution to Equation (1.1), where

$$|\mathcal{W}| < \mathcal{W}_{\max} = \frac{\pi}{\Delta\tau}, \tag{1.2}$$

and $\mathcal{W}_{\max}$ is the circular Nyquist frequency. From the physical standpoint, an envelope oscillation at frequency $\mathcal{W}$ is superimposed on the electric field oscillation at frequency ω_0, this is how the laboratory frequency $\omega = \omega_0 + \mathcal{W}$ comes into play. In the following, the frequency of a generic plane wave solution to GNLSE (1.1) is denoted by $\mathcal{W} = \nu$, the frequencies of its blue- and red-shifted satellites are $\mathcal{W} = \nu \pm \Omega$.

The characteristic function $D(\mathcal{W})$ of the linear dispersion operator $\mathfrak{D}$ in Equation (1.1) has its origin in the dispersion law, a dependence between the wave vector and the frequency of the background carrier fiber mode, $k = \beta(\omega)$. Specifically, the characteristic function describes how $\beta(\omega)$ deviates from a straight line in the vicinity of $\omega = \omega_0$

$$D(\mathcal{W}) = \beta(\omega_0 + \mathcal{W}) - \beta_0 - \beta_1\mathcal{W} \quad \text{with} \quad \beta_j = \left.\frac{d^j\beta(\omega)}{d\omega^j}\right|_{\omega=\omega_0}.$$

The characteristic function is usually approximated by a polynomial, which makes $\mathfrak{D}$ a differential operator

$$D(\mathcal{W}) = \sum_{j=2}^{J}\frac{\beta_j}{j!}\mathcal{W}^j, \quad \mathfrak{D} = \sum_{j=2}^{J}\frac{\beta_j}{j!}(i\partial_\tau)^j. \tag{1.3}$$

The summation starts at $j = 2$, because the contribution of β_0 and $\beta_1 = v_{\rm gr}^{-1}$ to the pulse evolution was eliminated in the derivation of Equation (1.1). The remaining beta coefficients are assumed to be known up to approximation order J.

A problem statement for Equation (1.1) is that the input pulse shape is known at the beginning of the fiber and its further evolution should be calculated along the fiber: given $\psi(z = 0, \tau)$ one looks for $\psi(z > 0, \tau)$. Physicists say

Equation (1.1) is unidirectional and z-propagated. The most famous member of the equations family (1.1) is the optical nonlinear Schrödinger equation with $J = 2$

$$i\partial_z\psi - \frac{\beta_2}{2}\partial_\tau^2\psi + \gamma|\psi|^2\psi = 0, \tag{1.4}$$

which is integrable [30]. Here, the pulse width in the frequency domain is so small that only β_2 counts in Equation (1.3). On the other hand, the further generalization of Equation (1.1) is necessary for spectrally broad ultrashort optical pulses to account for nonlinear dispersion and Raman scattering [8]. The paper deals with the numerical solution of the GNLSE (1.1) by split-step methods.

2 Numerical method

Equation (1.1) has clearly distinguishable terms of different nature. Namely, the linear operator $\mathfrak{D}$ appears because different spectral components of the input pulse propagate at different speeds, leading to dispersive pulse spreading [12]. The nonlinear term in Equation (1.1) is due to the nonlinear change in refractive index and leads to pulse compression and in extreme cases even to wave breaking [1,8]. As long as both dispersive and nonlinear effects are small, which was assumed in the derivation of Equation (1.1), a splitting scheme is a natural choice for the numerical solution. Of course, splitting methods are useful for many applications beyond the envelope equation, a recent book [10] contains several reviews of these applications. On the other hand, speaking specifically of envelope equations, several other solution methods are available, of which the splitting method is typically the fastest, see [17,24].

Using the simplest Lie-Trotter splitting method, one goes from $\psi(z = 0, \tau)$ to $\psi(z = h, \tau)$ in two substeps. The nonlinear part of Equation (1.1), $\partial_z\psi = i\gamma|\psi|^2\psi$, is solved first on $z \in [0, h]$. The result is used as an initial condition in the solution of the linear part, $\partial_z\psi = i\mathfrak{D}(\psi)$, again on $z \in [0, h]$ and typically employing two fast Fourier transforms. The result of the second substep is the required approximation for $\psi(z = h, \tau)$. The entire process is then repeated to approximate $\psi(z = 2h, \tau)$, and so on [1,27].

If we write the reduced equations for the linear and nonlinear substeps as $\partial_z\psi = B(\psi)$ and $\partial_z\psi = A(\psi)$ respectively, and if we denote the linear and nonlinear evolution operators by e^{hB} and e^{hA}, the simplest splitting method reads

$$\Psi(h, \tau) = e^{hB}e^{hA}\Psi(0, \tau) \quad \text{for} \quad \psi(h, \tau) = e^{h(B+A)}\psi(0, \tau).$$

In the above equations, Ψ denotes the split-step approximation of ψ and $e^{h(B+A)}$ represents the full evolution operator for Equation (1.1). Alternatively, the calculation can start with the linear substep followed by the nonlinear substep. Unless otherwise stated, we start with the nonlinear substep.

While the Lie-Trotter splitting is easy to implement, it still has its drawbacks. Its one-step accuracy is $O(h^2)$, indicating that the solution method is of first order. The accuracy can be improved by employing a higher-order splitting scheme. A general multiplicative splitting method, comprising of n stages,

with each stage consisting of a single nonlinear and linear substep, is defined by the approximation [18]

$$e^{h(B+A)} \approx e^{b_n hB} e^{a_n hA} \cdots e^{b_2 hB} e^{a_2 hA} e^{b_1 hB} e^{a_1 hA}. \tag{2.1}$$

The coefficients $a_{1\le s\le n}$ and $b_{1\le s\le n}$ are chosen such that the formal Taylor expansions of the left- and right-hand-side of Equation (2.1) coincide as good as possible. For instance, the well-known Suzuki-Yoshida splitting [23, 28] has 4 stages and one-step accuracy of $O(h^5)$, it provides a fourth-order method. Equation (2.1) can be easily understood for square matrices. Its relevance to the GNLSE, where e^{hA} involves a nonlinear operator A and e^{hB} involves an unbounded linear differential operator B, is discussed in [27]. Web page [3] includes a compilation of helpful splittings, for most of them the last substep is trivial ($b_n = 0$) such that one can omit $e^{a_n hA}$ and start the next iteration with $e^{(a_1+a_n)hA}$, effectively reducing the number of stages by 1.

A known drawback of splitting methods is that they may suffer from numerical instabilities due to their explicit nature. In the context of GNLSE, these instabilities are known to as the spurious instabilities [7, 16]. Weideman and Herbst [25] tackled this problem by exploiting the well-established physical phenomenon of (non-spurious) modulation instability [29] (MI). Namely, they considered an exact solution to Equation (1.4) for the constant-amplitude carrier wave

$$\psi = \sqrt{P_0} e^{i\gamma P_0 z}, \qquad P_0 = \text{const}, \tag{2.2}$$

which may ($\beta_2\gamma < 0$) or may not ($\beta_2\gamma > 0$) be prone to MI [1, 27]. Weideman and Herbst investigated to what extent this behavior is replicated by the Lie-Trotter splitting method and derived the necessary condition for the absence of spurious instabilities

$$h < \frac{2\pi}{|\beta_2| \mathcal{W}_{\max}^2}. \tag{2.3}$$

Here h is the numerical solution step and the spectrum of the approximate GNLSE solution $\Psi(z, \tau)$ is bounded by $\mathcal{W}_{\max}$ in accord with Equation (1.2).

The method that leads to Equation (2.3) can be generalized in several directions. One could (i) explore other solutions of the integrable Equation (1.4), (ii) consider the more general Equation (1.1), which serves as a standard model in nonlinear fiber optics, and (iii) explore an arbitrary splitting. The first [14,15] and second [15, 22] approaches have been discussed in the literature, while for the third approach we are only aware on studies of the Suzuki-Yoshida splitting method [27]. In the following, we will discuss the spurious instabilities in regard to Equation (1.1) and an arbitrary splitting method.

3 Modulation instability

This section presents essential information regarding MI, which must be accurately reproduced by a numerical solution of Equation (1.1). For the full description the reader should consult standard textbooks [1, 27]. We consider a specific subset of solutions to Equation (1.1)

$$\psi(z, \tau) = \left(\sqrt{P_0} + \widetilde{\psi}(z, \tau)\right) e^{i(D(\nu)+\gamma P_0)z - i\nu\tau}, \quad \text{where} \quad |\widetilde{\psi}| \ll \sqrt{P_0}. \tag{3.1}$$

For $\widetilde{\psi} = 0$, Equation (3.1) yields an exact solution to Equation (1.1). The solution describes a wave with a constant amplitude $\sqrt{P_0}$, its laboratory frequency is $\omega_0 + \nu$. Note, that γP_0 is the nonlinear wave vector shift. In what follows, the dimensionless value of $h\gamma P_0$ will play an important role for a numerical solution with the evolution step h.

The most natural selection in Equation (3.1) is $\nu = 0$, bringing us back to the solution (2.2). Waves with $\nu \neq 0$ can occur due to inaccurate carrier frequency selection, when several waves with slightly different frequencies are described by one envelope equation, or due to various physical phenomena such as nonlinear wave interactions [13] and self-frequency shift [11, 19]. This holds particularly true for the optical supercontinuum state [9].

With a small but non-zero $\widetilde{\psi}$, we can study the stability of the carrier wave. Substituting Equation (3.1) into Equation (1.1) and keeping the first order terms, we obtain a linear equation

$$i\partial_z \widetilde{\psi} + e^{i\nu\tau}\mathfrak{D}(\widetilde{\psi}e^{-i\nu\tau}) - D(\nu)\widetilde{\psi} + \gamma P_0(\widetilde{\psi} + \widetilde{\psi}^*) = 0. \tag{3.2}$$

Equation (3.2) has a collection of partial solutions that are parameterized by a real parameter Ω

$$\widetilde{\psi}(z,\tau) = u(z)e^{-i\Omega\tau} + v^*(z)e^{i\Omega\tau}. \tag{3.3}$$

From a physical standpoint, two additional waves arise at $\omega = \omega_0 + \nu \pm \Omega$. They are identified as the blue- and red-shifted MI satellites and in accord with Equation (3.2) can be found from the system

$$\partial_z \begin{bmatrix} u \\ v \end{bmatrix} = i \begin{bmatrix} N_\nu(\Omega) + M_\nu(\Omega) + \gamma P_0 & \gamma P_0 \\ -\gamma P_0 & N_\nu(\Omega) - M_\nu(\Omega) - \gamma P_0 \end{bmatrix} \begin{bmatrix} u \\ v \end{bmatrix}. \tag{3.4}$$

Here we introduce notations

$$\begin{aligned} M_\nu(\Omega) &= \frac{D(\nu+\Omega) - 2D(\nu) + D(\nu-\Omega)}{2}, \\ N_\nu(\Omega) &= \frac{D(\nu+\Omega) - D(\nu-\Omega)}{2}, \end{aligned} \tag{3.5}$$

which bear some resemblance to the definitions of discrete derivatives. $M_\nu(\Omega)$ is referred to as mismatch. The right-hand-side of Equation (3.4) yields two eigenvalues

$$\lambda = iN_\nu(\Omega) \pm \sqrt{-M_\nu(\Omega)(M_\nu(\Omega) + 2\gamma P_0)},$$

and MI takes place if

$$M_\nu(\Omega)(M_\nu(\Omega) + 2\gamma P_0) < 0 \quad \Rightarrow \quad M_\nu(\Omega) \in (-2\gamma P_0, 0), \tag{3.6}$$

where the final implication uses $\gamma > 0$. In a favorable situation (e.g., for $D''(\nu) < 0$), Equation (3.6) yields several domains on Ω axis, the domains are translated into growing perturbations (3.3) indicating presence of the instability. The numerical solution should display these domains up to some approximation, moreover, it should not display any additional domains.

4 Split-step approach to modulation instability

To facilitate a comparison between the continuous and discrete solutions of GNLSE, we follow [22] and rephrase the well-known results from the previous section. It is convenient to use the matrix form of both Equation (3.4)

$$\partial_z \begin{bmatrix} u \\ v \end{bmatrix} = i(N_\nu(\Omega)\mathbf{I} + M_\nu(\Omega)\mathbf{J} + \gamma P_0 \mathbf{K}) \begin{bmatrix} u \\ v \end{bmatrix}, \tag{4.1}$$

and its solution

$$\begin{bmatrix} u(z) \\ v(z) \end{bmatrix} = e^{iz(N_\nu(\Omega)\mathbf{I}+M_\nu(\Omega)\mathbf{J}+\gamma P_0\mathbf{K})} \begin{bmatrix} u(0) \\ v(0) \end{bmatrix}, \tag{4.2}$$

where

$$\mathbf{I} = \begin{bmatrix} 1 & 0 \\ 0 & 1 \end{bmatrix}, \quad \mathbf{J} = \begin{bmatrix} 1 & 0 \\ 0 & -1 \end{bmatrix}, \quad \mathbf{K} = \begin{bmatrix} 1 & 1 \\ -1 & -1 \end{bmatrix}.$$

For an integration step, Equation (4.2) yields the following exact expression

$$\begin{bmatrix} u(z+h) \\ v(z+h) \end{bmatrix} = e^{ihN_\nu(\Omega)} e^{ih(M_\nu(\Omega)\mathbf{J}+\gamma P_0\mathbf{K})} \begin{bmatrix} u(z) \\ v(z) \end{bmatrix}. \tag{4.3}$$

Note, that the determinant of $e^{ih(M_\nu(\Omega)\mathbf{J}+\gamma P_0\mathbf{K})}$ is 1 and therefore the instability condition is

$$\left| \mathrm{Tr}\left(e^{ih(M_\nu(\Omega)\mathbf{J}+\gamma P_0\mathbf{K})} \right) \right| > 2. \tag{4.4}$$

It is not difficult to obtain $e^{ih(M_\nu(\Omega)\mathbf{J}+\gamma P_0\mathbf{K})}$ explicitly, which brings Equation (4.4) back to the criterion (3.6).

The above approach can be used with any splitting method. Indeed, Equation (4.1) contains terms that come from linear and nonlinear parts of GNLSE. By treating them separately, we see that an arbitrary splitting (2.1) corresponds to the following approximation

$$\begin{bmatrix} U(z+h) \\ V(z+h) \end{bmatrix} = e^{ihN_\nu(\Omega)} \left(\prod_{n \geq s \geq 1} e^{ib_s h M_\nu(\Omega)\mathbf{J}} e^{ia_s h \gamma P_0 \mathbf{K}} \right) \begin{bmatrix} U(z) \\ V(z) \end{bmatrix}, \tag{4.5}$$

where U and V approximate u and v from Equation (4.3). The difference between the exact Equation (4.3) and its split-step approximation (4.5) appears because $\mathbf{JK} \neq \mathbf{KJ}$. Determinant of the matrix product in Equation (4.5) is still 1, such that the inequality

$$\left| \mathrm{Tr} \left(\prod_{n \geq s \geq 1} e^{ib_s h M_\nu(\Omega)\mathbf{J}} e^{ia_s h \gamma P_0 \mathbf{K}} \right) \right| > 2, \tag{4.6}$$

is the split-step approximation of the MI condition (4.4).

To proceed with Equation (4.6), it is convenient to introduce two dimensionless parameters

$$\varepsilon = h\gamma P_0, \quad \phi = h M_\nu(\Omega). \tag{4.7}$$

In fiber optics, the quantity $(\gamma P_0)^{-1}$ is referred to as nonlinear length and indicates the propagation distance at which nonlinear effects become significant [1]. In any case, the numerical solution step h should be smaller than the nonlinear length and therefore Equation (4.6) can be simplified using $\varepsilon \ll 1$. On the other hand, the value of ϕ can be arbitrary, because "small" h is multiplied by a polynomial $M_\nu(\Omega)$ with possibly "large" Ω. In addition, we introduce the notations

$$b_{pq} = \begin{cases} b_{p-1} + b_{p-2} + \cdots + b_q & \text{if } p > q, \\ 1 - b_{qp} & \text{if } q > p, \end{cases} \tag{4.8}$$

and

$$\sum_{p,q,\ldots r}{}' = \sum_{n \geq p > q > \cdots > r \geq 1}, \tag{4.9}$$

where summation in the last expression is over all possible values of its indices from n to 1 subject to the specified inequality. The trace in Equation (4.6) is calculated in the Appendix A, the result reads

$$\begin{aligned} \mathrm{Tr}\left(\prod_{n\geq s\geq 1} e^{ib_s\phi\mathbf{J}} e^{ia_s\varepsilon\mathbf{K}}\right) &= 2\cos(\phi) - 2\varepsilon\sin(\phi) + 4\varepsilon^2 \sum_{p,q}{}' a_p a_q \sin(b_{pq}\phi)\sin(b_{qp}\phi) \\ &- 8\varepsilon^3 \sum_{p,q,r}{}' a_p a_q a_r \sin(b_{pq}\phi)\sin(b_{qr}\phi)\sin(b_{rp}\phi) \\ &+ 16\varepsilon^4 \sum_{p,q,r,s}{}' a_p a_q a_r a_s \sin(b_{pq}\phi)\sin(b_{qr}\phi)\sin(b_{rs}\phi)\sin(b_{sp}\phi) + \cdots \end{aligned} \tag{4.10}$$

Applications of this result will be given in the next section. The first nontrivial term of the expansion (4.10) was previously calculated in [21]. Splitting methods that start with a linear substep are discussed in the Appendix B.

5 Examples

Equations (4.6) and (4.10) represent the primary outcome of the paper and make it possible to analyze the interplay of the MI and spurious instabilities. Note, that they were obtained by going from $\psi(z,\tau)$ to $\psi(z+h,\tau)$ by an arbitrary splitting method, where the τ variable still is continuous. We will now examine this situation in more detail, and discuss what happens due to the discretization of the retarded time.

True MI. Recall that $\varepsilon > 0$ is a small parameter, while ϕ does not have to be small, as discussed after Equation (4.7). If nevertheless we consider the case that $\phi = O(\epsilon)$, Equation (4.6) yields

$$|2 - \phi(\phi + 2\varepsilon) + O(\varepsilon^4)| > 2.$$

This is compatible with the MI condition (3.6), which translates into inequality $\phi(\phi + 2\varepsilon) < 0$. The resulting MI domain $\phi \in (-2\varepsilon, 0)$ is compatible with the assumption that $\phi = O(\epsilon)$. Therefore the core MI is correctly described by

any splitting method as long as $\varepsilon \ll 1$. An arbitrary ϕ is another story, this is where the spurious instabilities occur.

Lie-Trotter and Strang splittings. For both $e^{h(B+A)} \approx e^{hB}e^{hA}$ (Lie-Trotter) and $e^{h(B+A)} \approx e^{\frac{h}{2}A}e^{hB}e^{\frac{h}{2}A}$ (Strang) splitting methods, the instability condition (4.6) reduces to

$$|\cos(\phi) - \varepsilon \sin(\phi)| > 1.$$

The inequality also applies to the Lie-Trotter and Strang methods that begin with a linear substep. It was first derived in the pioneer paper [25]. The function on the left-hand-side takes its maximal value $\sqrt{1+\varepsilon^2}$ for

$$\phi = \phi_m = \pi m - \arctan\varepsilon, \quad m \in \mathbb{Z}.$$

Each such ϕ_m is in the middle of its instability domain

$$\phi \in I_m = (\pi m - 2\arctan\varepsilon, \pi m).$$

The true MI domain (3.6), which is $\phi \in (-2\varepsilon, 0)$, is approximately recovered for $m = 0$, as expected from the previous subsection. The remaining domains are associated with spurious instabilities and should be avoided. There are two obvious ways to remove them.

First, any discrete in τ approximation of $\psi(z = nh, \tau)$ has a finite bandwidth such that both satellite frequencies $\mathcal{W} = \nu \pm \Omega$ must be smaller that $\mathcal{W}_{\max}$ from Equation (1.2). This condition on Ω can be used to estimate the polynomial mismatch $M_\nu(\Omega)$, i.e., to find an upper bound of $\phi = hM_\nu(\Omega)$. The range of the possible ϕ values should be chosen so that it includes I_0 and has no intersections with $I_{\pm 1}$. It is sufficient to require

$$-\pi < \phi < \pi - 2\arctan\varepsilon, \tag{5.1}$$

which is achieved by decreasing h. For simplicity, one can write the last inequality as $|\phi| < \pi$ and take its predictions with a grain of salt. For instance, for the nonlinear Schrödinger equation (1.4), the inequality (5.1) reduces to

$$-\pi < \frac{h\beta_2\Omega^2}{2} < \pi \quad \text{for} \quad |\nu \pm \Omega| < \mathcal{W}_{\max},$$

and leads to the classical condition (2.3) for $\nu = 0$. Applications of this approach to GNLSE were discussed in [15, 22]. Another possibility is to study whether the spurious instability domains can be removed by a more accurate splitting method using the general criterion (4.6). This will be done bellow.

A generic two-stage splitting. Consider the approximation

$$e^{h(A+B)} \approx e^{hb_2B}e^{ha_2A}e^{hb_1B}e^{ha_1A}, \quad a_1 + a_2 = 1, \quad b_1 + b_2 = 1.$$

Its local accuracy is $O(h^2)$, the accuracy becomes $O(h^3)$ if $a_2b_1 = 1/2$. Strang splitting belongs to this class, as well as the best-two-stage splitting

$$e^{h(B+A)} \approx e^{\left(1-\frac{\sqrt{2}}{2}\right)hB}e^{\frac{\sqrt{2}}{2}hA}e^{\frac{\sqrt{2}}{2}hB}e^{\left(1-\frac{\sqrt{2}}{2}\right)hA},$$

and the rational Milne splitting

$$e^{h(B+A)} \approx e^{\frac{h}{5}B} e^{\frac{5h}{8}A} e^{\frac{4h}{5}B} e^{\frac{3h}{8}A},$$

see [3]. Using Equation (4.10), one derives the instability criterion

$$|\cos(\phi) - \varepsilon \sin(\phi) + 2a_1 a_2 \varepsilon^2 \sin(b_1\phi) \sin(b_2\phi)| > 1,$$

which yields the true MI for $\phi = O(\varepsilon)$, and the spurious instabilities in the vicinity of $\phi = \pm\pi$. It is easy to see that the spurious instabilities can be reduced to some extent, a close to optimal choice is

$$e^{h(B+A)} \approx e^{-\frac{h}{2}B} e^{\frac{h}{3}A} e^{\frac{3h}{2}B} e^{\frac{2h}{3}A}.$$

However, the spurious instabilities are still present. The only exception is a trivial first-order two-stage splitting $e^{\frac{h}{2}B} e^{\frac{h}{2}A} e^{\frac{h}{2}B} e^{\frac{h}{2}A}$, in which case they appear in the vicinity of $\phi = \pm 2\pi$, because the integration step h is actually halved.

Higher-order splittings. Now we consider two practically relevant 4th and 6th order splittings with $n = 7$ and $n = 11$ respectively, namely S_6 and S_{10} methods with effectively 6 and 10 stages developed by Blanes and Moan [6]. As the analytical approach seems to be impossible here, the left-hand-side of Equation (4.6) is numerically plotted in Figure 1. In addition, we show the results for the classical Suzuki-Yoshida splitting. The latter is even worse than the simplest Lie-Trotter method when one starts with a nonlinear substep, see [27]. As to S_6 and S_{10} splittings, the spurious instabilities are strongly suppressed for both of them, but they still exist in extremely narrow domains at $\phi = \pm\pi$.

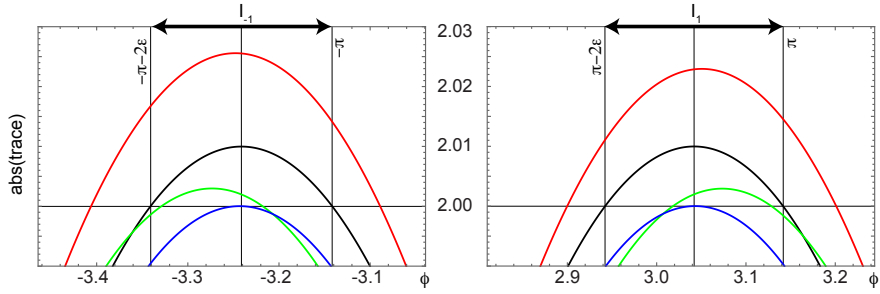

Figure 1. Left-hand-side of Equation (4.6) is shown upon $\phi \in I_{-1}$ (left panel) and $\phi \in I_1$ (right panel) for $\varepsilon = 0.1$ and several popular splitting methods. The spurious instabilities appear where |trace| > 2. The following methods are presented: Lie-Trotter (black, the same curve also applies to the Strang splitting), Suzuki-Yoshida (red), Suzuki-Yoshida starting with the linear substep (green), S_6 and S_{10} methods reported by Blanes and Moan [6] (both blue, the difference between the methods is too small to see). The latter two methods seem to be free of the spurious instabilities, but actually have eigenvalues that exceed 1 by a small amount ($\lambda - 1 \approx 4 \cdot 10^{-3}$ for S_6 and $2 \cdot 10^{-4}$ for S_{10}).

To illustrate this, consider a GNLSE that applies to the so-called *pure-quartic solitons*

$$i\partial_z\psi + \frac{\beta_4}{24}\partial_\tau^4\psi + \gamma|\psi|^2\psi = 0, \tag{5.2}$$

see [5]. Equation (5.2) has a constant-amplitude carrier wave solution (2.2), the latter is stable if $\beta_4\gamma > 0$. Let us consider to which extent this property is reproduced by the 6th order split-step method S_{10} from [6]. Figure 2 shows two numerical solutions of Equation (5.2) for a randomly perturbed wave (2.2). The solution step is taken slightly below and slightly above the value predicted by the inequality (5.1). As we see, the numerical instability is not eliminated by use of an accurate higher-order splitting method. One still has to reduce the integration step.

Note, that the initial field state that was used to generate Figure 2 corresponds to the plain-wave solution of GNLSE, the one that was used to analyze MI. Extending of these results to an arbitrary solution of GNLSE is a complicated problem beyond the scope of the present study. To the best of our knowledge, it has only been addressed for a fundamental soliton solution in the simplest integrable NLSE, see [14].

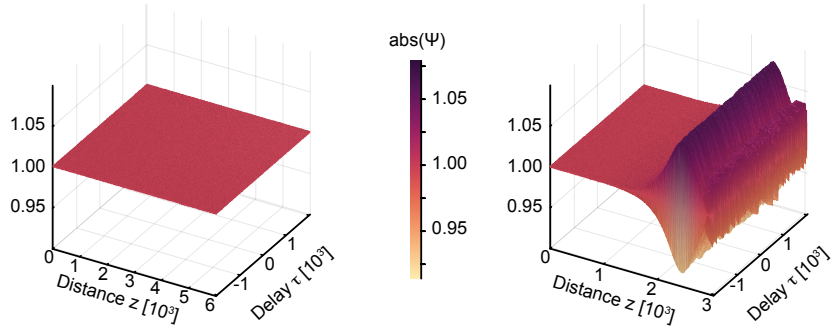

Figure 2. Two exemplary numerical solutions of the GNLSE (5.2) with $\beta_4 = 0.05$ and $\gamma = 0.2$. A mathematically stable initial condition (2.2) with $P_0 = 1$ was used. The constant-amplitude wave was randomly perturbed, the perturbation level was 0.1 %. An accurate 6th-order split-step method S_{10} from [6] was applied with $\Delta\tau = 0.25$ and 2^{14} harmonics. The left panel shows 10^5 steps with $h = 0.060$. The right panel shows $5 \cdot 10^4$ steps with $h = 0.061$. The results agree with the inequality (5.1), the latter for the case at hand predicts spurious instabilities for the integration step $h > 0.06047$.

6 Conclusions

As explained when analyzing the Lie-Trotter and Strang splittings in Section 5, a sure way to eliminate the spurious instabilities is to impose a restriction onto the mismatch (3.5). Roughly speaking, it is necessary that $h|M_\nu(\Omega)| < \pi$, for all carrier offsets ν and all satellite offsets Ω, for more details see [15, 22]. The main result of the present study is that:

- The requirement $h|M_\nu(\Omega)| < \pi$ holds true for all tested splitting methods, no matter how accurate the splitting is.

Using more and more accurate splitting schemes, one still faces the spurious instabilities (Figure 1). As the approximation order increases, the instabilities tend to become less pronounced, moreover their domain may become extremely narrow, as it happens for the S_6 and S_{10} splittings from [6]. In practice, there are good chances that discrete numerical frequencies does not hit the unstable domain, or that the spurious instability will not have time to develop on a finite integration interval, see Figure 2. Nevertheless, the spurious instabilities are present. This leads to a conclusion, that

- A higher-order splitting method can be used to make calculations more accurate with the same h, but it cannot be used to make calculations more fast by employing a considerably larger h.

To avoid the spurious instabilities, the derivation of splitting schemes should be reconsidered. One should take care that the trace in Equation (4.6) do not exceed 2 when choosing coefficients of a splitting method. We can hope that it is possible, e.g., because for a trivial two-stage splitting $e^{\frac{h}{2}B}e^{\frac{h}{2}A}e^{\frac{h}{2}B}e^{\frac{h}{2}A}$, which is used in certain additive schemes [2], the spurious instabilities first appear at $h|M_\nu(\Omega)| \approx 2\pi$. One should look for new higher-order splittings with the same property. This will be a topic for future research.

References

[1] G. P. Agrawal. *Nonlinear Fiber Optics*. Academic, New York, 4 edition, 2007.

[2] Sh. Amiranashvili, M. Radziunas, U. Bandelow, K. Busch and R. Čiegis. Additive splitting methods for parallel solutions of evolution problems. *Journal of Computational Physics*, **436**(110320):1–14, July 2021. https://doi.org/10.1016/j.jcp.2021.110320.

[3] W. Auzinger, H. Hofstätter and O. Koch. Coefficients of various splitting methods. `https://www.asc.tuwien.ac.at/~winfried/splitting/`.

[4] M. Bass, E. W. Van Stryland, D. R. Williams and W. L. Wolfe (Eds.). *Handbook of Optics*, volume 1. McGRAW-HILL, 2 edition, 1995.

[5] A. Blanco-Redondo, C.M. de Sterke, J.E. Sipe, T.F. Krauss, B.J. Eggleton and C. Husko. Pure-quartic solitons. *Nat. Commun.*, **7**(10427):1–9, January 2016. https://doi.org/10.1038/ncomms10427.

[6] S. Blanes and P.C. Moan. Practical symplectic partitioned Runge-Kutta and Runge-Kutta-Nyström methods. *Journal of Computational and Applied Mathematics*, **142**(2):313–330, May 2002. https://doi.org/10.1016/S0377-0427(01)00492-7.

[7] G. Bosco, A. Carena, V. Curri, R. Gaudino, P. Poggiolini and S. Benedetto. Suppression of spurious tones induced by the split-step method in fiber systems simulation. *IEEE Photonics Technology Letters*, **13**(5):489–491, May 2000. https://doi.org/10.1109/68.841262.

[8] R. W. Boyd. *Nonlinear Optics*. Academic, New York, 3 edition, 2008.

[9] J. M. Dudley, G. Genty and S. Coen. Supercontinuum generation in photonic crystal fiber. *Rev. Mod. Phys.*, **78**(4):1135–1184, 2006. https://doi.org/10.1103/RevModPhys.78.1135.

[10] Roland Glowinski, Stanley J. Osher and Wotao Yin (Eds.). *Splitting Methods in Communication, Imaging, Science, and Engineering*. Scientific Computation. Springer, Berlin, 2016.

[11] J.P. Gordon. Theory of the soliton self-frequency shift. *Opt. Lett.*, **11**(10):662–664, October 1986. https://doi.org/10.1364/OL.11.000662.

[12] V. I. Karpman. *Non-linear waves in dispersive media*. Pergamon, 1975.

[13] E. Kartashova. *Nonlinear Resonance Analysis*. Cambridge University Press, 2010.

[14] T.I. Lakoba. Instability analysis of the split-step Fourier method on the background of a soliton of the nonlinear Schrödinger equation. *Numerical Methods for Partial Differential Equations*, **28**(2):641–669, March 2012. https://doi.org/10.1002/num.20649.

[15] T.I. Lakoba. Instability of the split-step method for a signal with nonzero central frequency. *J. Opt. Soc. Am. B*, **30**(12):3260–3271, December 2013. https://doi.org/10.1364/JOSAB.30.003260.

[16] T.I. Lakoba. Long-time simulations of nonlinear Schrödinger-type equations using step size exceeding threshold of numerical instability. *J Sci Comput*, **72**(1):14–48, July 2017. https://doi.org/10.1007/s10915-016-0346-y.

[17] Martino Lovisetto, Didier Clamond and Bruno Marcos. Integrating factor techniques applied to the Schrödinger-like equations. Comparison with Split-Step methods. *Applied Numerical Mathematics*, **197**:258–271, March 2024. https://doi.org/10.1016/j.apnum.2023.11.016.

[18] R.I. McLachlan and R. Quispel. Splitting methods. *Acta Numerica*, **11**:341–434, January 2002. https://doi.org/10.1017/S0962492902000053.

[19] F.M. Mitschke and L.F. Mollenauer. Discovery of the soliton self-frequency shift. *Opt. Lett.*, **11**(10):569–661, 1986. https://doi.org/10.1364/OL.11.000659.

[20] A. H. Nayfeh. *Perturbation methods*. Wiley, 1973.

[21] F. Severing, U. Bandelow and Sh. Amiranashvili. Spurious four-wave mixing processes in generalized nonlinear Schrödinger equations. Preprint 2975, WIAS, Mohrenstr. 39, 10117 Berlin, November 2022. Available on Internet: `https://www.wias-berlin.de/preprint/2975/wias_preprints_2975.pdf`

[22] F. Severing, U. Bandelow and Sh. Amiranashvili. Spurious four-wave mixing processes in generalized nonlinear Schrödinger equations. *J. Lightwave Technol.*, **41**(16):5359–5365, August 2023. https://doi.org/10.1109/JLT.2023.3261804.

[23] M. Suzuki. Fractal decomposition of exponential operators with applications to many-body theories and Monte Carlo simulations. *Phys. Lett. A*, **146**(6):319–323, June 1990. https://doi.org/10.1016/0375-9601(90)90962-N.

[24] T.R. Taha and M.I. Ablowitz. Analytical and numerical aspects of certain nonlinear evolution equations. II. Numerical, nonlinear Schrödinger equation. *Journal of Computational Physics*, **55**(2):231–253, August 1984. https://doi.org/10.1016/0021-9991(84)90003-2.

[25] J.A.C. Weideman and B.M. Herbst. Split-Step methods for the solution of the nonlinear Schrödinger equation. *SIAM J. Numer. Anal.*, **23**(3):485–507, June 1986. https://doi.org/10.1137/0723033.

[26] G. B. Whitham. *Linear and nonlinear waves*. John Wiley & Sons, New York, 1974.

[27] J. Yang. *Nonlinear Waves in Integrable and Nonintegrable Systems*. SIAM, 2010.

[28] H. Yoshida. Construction of higher order symplectic integrators. *Phys. Lett. A*, **150**(5-7):262–268, November 1990. https://doi.org/10.1017/S0074180900091440.

[29] V.E. Zakharov and L.A. Ostrovsky. Modulation instability: the beginning. *Physica D: Nonlinear Phenomena*, **238**(5):540–548, March 2009. https://doi.org/10.1016/j.physd.2008.12.002.

[30] V.E. Zakharov and A.B. Shabat. Exact theory of two-dimensional self-focusing and one-dimensional self-modulation of waves in nonlinear media. *Sov. Phys. JETP*, **34**(1):62–69, 1972.

Appendix A. Trace calculation

The derivation of Equation (4.10) is outlined in this Appendix. We consider the matrix from Equation (4.6), the matrix will be denoted by $\mathbf{U}$, and use the notations from Equation (4.7) such that

$$\mathbf{U} = \prod_{n\geq s\geq 1} e^{ib_s\phi\mathbf{J}} e^{ia_s\varepsilon\mathbf{K}} = \begin{bmatrix} e^{ib_n\phi} & 0 \\ 0 & e^{-ib_n\phi} \end{bmatrix} (\mathbf{I} + ia_n\varepsilon\mathbf{K}) \cdots \begin{bmatrix} e^{ib_1\phi} & 0 \\ 0 & e^{-ib_1\phi} \end{bmatrix} (\mathbf{I} + ia_1\varepsilon\mathbf{K}),$$

because $\mathbf{K}^2 = 0$. Calculating $\mathbf{U}$, it is natural to introduce an expansion

$$\mathbf{U} = \begin{bmatrix} e^{i\phi} & 0 \\ 0 & e^{-i\phi} \end{bmatrix} + \varepsilon\mathbf{U}^{(1)} + \varepsilon^2\mathbf{U}^{(2)} + \varepsilon^3\mathbf{U}^{(3)} + \cdots,$$

because in all practically relevant cases $\varepsilon \ll 1$, as explained after Equation (4.7). We have the following expressions

$$\mathbf{U}^{(1)} = \sum_{n\geq p\geq 1} \begin{bmatrix} e^{i(b_n+\cdots b_p)\phi} & 0 \\ 0 & e^{-i(b_n+\cdots b_p)\phi} \end{bmatrix} (ia_p\mathbf{K}) \times \begin{bmatrix} e^{i(b_{p-1}+\cdots b_1)\phi} & 0 \\ 0 & e^{-i(b_{p-1}+\cdots b_1)\phi} \end{bmatrix},$$

and

$$\mathbf{U}^{(2)} = \sum_{n\geq p>q\geq 1} \begin{bmatrix} e^{i(b_n+\cdots b_p)\phi} & 0 \\ 0 & e^{-i(b_n+\cdots b_p)\phi} \end{bmatrix} (ia_p\mathbf{K}) \times \begin{bmatrix} e^{i(b_{p-1}+\cdots b_q)\phi} & 0 \\ 0 & e^{-i(b_{p-1}+\cdots b_q)\phi} \end{bmatrix} (ia_q\mathbf{K}) \times \begin{bmatrix} e^{i(b_{q-1}+\cdots b_1)\phi} & 0 \\ 0 & e^{-i(b_{q-1}+\cdots b_1)\phi} \end{bmatrix},$$

and

$$\begin{aligned}\mathbf{U}^{(3)} = \sum_{n\geq p>q>r\geq 1} &\begin{bmatrix} e^{i(b_n+\cdots b_p)\phi} & 0 \\ 0 & e^{-i(b_n+\cdots b_p)\phi}\end{bmatrix}(ia_p\mathbf{K}) \\ &\times\begin{bmatrix} e^{i(b_{p-1}+\cdots b_q)\phi} & 0 \\ 0 & e^{-i(b_{p-1}+\cdots b_q)\phi}\end{bmatrix}(ia_q\mathbf{K}) \\ &\times\begin{bmatrix} e^{i(b_{q-1}+\cdots b_r)\phi} & 0 \\ 0 & e^{-i(b_{q-1}+\cdots b_r)\phi}\end{bmatrix}(ia_r\mathbf{K}) \\ &\times\begin{bmatrix} e^{i(b_{r-1}+\cdots b_1)\phi} & 0 \\ 0 & e^{-i(b_{r-1}+\cdots b_1)\phi}\end{bmatrix},\end{aligned}$$

with the evident structure of the further terms. Using a cyclic permutation of the first multiplier and the shortcuts from Equation (4.8) and (4.9), we see that as long as only traces of the above matrices are of interest, it is possible to make the following replacements

$$\begin{aligned}\mathbf{U}^{(1)} &\mapsto \sum_{n\geq p\geq 1}(ia_p\mathbf{K})\begin{bmatrix} e^{i\phi} & 0 \\ 0 & e^{-i\phi}\end{bmatrix}, \\ \mathbf{U}^{(2)} &\mapsto \sum_{p,q}{}'(ia_p\mathbf{K})\begin{bmatrix} e^{ib_{pq}\phi} & 0 \\ 0 & e^{-ib_{pq}\phi}\end{bmatrix}(ia_q\mathbf{K})\begin{bmatrix} e^{ib_{qp}\phi} & 0 \\ 0 & e^{-ib_{qp}\phi}\end{bmatrix}, \\ \mathbf{U}^{(3)} &\mapsto \sum_{p,q,r}{}'(ia_p\mathbf{K})\begin{bmatrix} e^{ib_{pq}\phi} & 0 \\ 0 & e^{-ib_{pq}\phi}\end{bmatrix}(ia_q\mathbf{K})\begin{bmatrix} e^{ib_{qr}\phi} & 0 \\ 0 & e^{-ib_{qr}\phi}\end{bmatrix} \\ &\quad\times(ia_r\mathbf{K})\begin{bmatrix} e^{ib_{rp}\phi} & 0 \\ 0 & e^{-ib_{rp}\phi}\end{bmatrix}, \\ \mathbf{U}^{(4)} &\mapsto \sum_{p,q,r,s}{}'(ia_p\mathbf{K})\begin{bmatrix} e^{ib_{pq}\phi} & 0 \\ 0 & e^{-ib_{pq}\phi}\end{bmatrix}(ia_q\mathbf{K})\begin{bmatrix} e^{ib_{qr}\phi} & 0 \\ 0 & e^{-ib_{qr}\phi}\end{bmatrix} \\ &\quad\times(ia_r\mathbf{K})\begin{bmatrix} e^{ib_{rs}\phi} & 0 \\ 0 & e^{-ib_{rs}\phi}\end{bmatrix}(ia_s\mathbf{K})\begin{bmatrix} e^{ib_{sp}\phi} & 0 \\ 0 & e^{-ib_{sp}\phi}\end{bmatrix},\end{aligned}$$

and so on. With the help of some computer algebra, traces of the latter expressions finally lead to the expansion (4.10). We also calculated $\mathbf{U}^{(5)}$ and $\mathbf{U}^{(6)}$, their contribution preserves the general structure of Equation (4.10).

Appendix B. Splitting methods that start with a linear substep

Recall, that the evolution operators triggered by the linear and nonlinear substeps were denoted by e^{hB} and e^{hA}, i.e., Equation (2.1) describes a generic splitting method that starts with a nonlinear substep. If one chooses to start with a linear substep, Equation (2.1) should be replaced by

$$e^{h(B+A)} \approx e^{b_nhA}e^{a_nhB}\ \cdots\ e^{b_2hA}e^{a_2hB}e^{b_1hA}e^{a_1hB}, \tag{B.1}$$

and the reformulated Equation (4.6) is

$$\left| \mathrm{Tr} \left(\prod_{n \geq s \geq 1} e^{ib_s h \gamma P_0 \mathbf{K}} e^{ia_s h M_\nu(\Omega) \mathbf{J}} \right) \right| > 2.$$

The latter inequality gets the same structure as the original Equation (4.6) after a cyclic permutation that moves the last exponent to the first place, the trace is not affected. Therefore we can take any relation derived from Equation (4.6), apply the replacement rule

$$b_n, a_n, b_{n-1}, a_{n-1} \cdots b_2, a_2, b_1, a_1 \quad \mapsto \quad a_1, b_n, a_n, b_{n-1} \cdots a_3, b_2, a_2, b_1,$$

and get the linked result for the splitting method (B.1). The practical difference between the splittings (2.1) and (B.1) can be quite significant, see Figure 1.